$[Ru_6C(CO)_{17}]$: A Case of Organometallic Crystal Polymorphism†

Dario Braga,[a] Fabrizia Grepioni,*[,a] Paul J. Dyson,[b] Brian F. G. Johnson,[b] Piero Frediani,[c] Mario Bianchi[c] and Franco Piacenti[c]

[a] *Dipartimento di Chimica 'G. Ciamician', Università di Bologna, Via Selmi 2, 40126 Bologna, Italy*
[b] *Department of Chemistry, University of Edinburgh, West Mains Road, Edinburgh EH9 3JJ, UK*
[c] *Dipartimento di Chimica Organica, Università di Firenze, Via Gino Capponi 9, 50121 Firenze, Italy*

The molecular structure of the prototypical hexaruthenium carbidocarbonyl cluster $[Ru_6C(CO)_{17}]$ has been redetermined on crystals obtained by two different routes. Form **I** is monoclinic, space group $P2_1/n$, $a = 9.19(1)$, $b = 32.043(9)$, $c = 9.598(4)$ Å, $\beta = 111.93(3)°$, $Z = 4$, $R = 0.076$, $R' = 0.079$, for 2764 $[I_o > 2\sigma(I_o)]$ out of 4755 absorption-corrected reflections; form **II** is also monoclinic, space group $P2/a$, $a = 17.668(2)$, $b = 9.335(1)$, $c = 24.057(7)$ Å, $\beta = 97.96(2)°$, $Z = 6$, $R = 0.023$, $R' = 0.028$, for 7656 $[I_o > 2\sigma(I_o)]$ out of 10 288 absorption-corrected reflections. The structural analysis shows that the complex possesses three different molecular structures in the solid state (**I**, **IIA** and **IIB**), differing essentially in the rotameric conformation of the tricarbonyl units above and below the equatorial plane containing bridging and semibridging ligands. The conformation is staggered in form **I**, while **II** contains two nearly eclipsed conformers. The relationship between the structure of the three isomers and of their crystals has been investigated.

Many organic molecules are known to crystallize as polymorphs and an abundant literature is available on crystalline organic materials. Much of what is known on polymorphism is due to the continuing efforts of Bernstein and co-workers.[1] The accumulation of a large base of structural data has revealed that the occurrence of polymorphism is a widespread phenomenon in solid-state organic chemistry.[2]

Studies of crystal polymorphism are very informative on the effect of packing forces on the molecular structure observed in the solid state. 'Packing forces' are often invoked to account for relevant deviations from idealized molecular structure or for unexpected structural features. Recently, crystal-packing effects on molecular structures have been clearly recognized in a number of organometallic crystals of mono- and poly-nuclear complexes.[3] Although much progress has been made in recent years in the understanding of the crystal packing of molecules, the nature of these forces is still quite elusive. The molecular structure of flexible molecules in the solid state is not necessarily *a priori* identical to that in solution or in the gas phase. It has been shown in several cases that crystal forces can 'compensate for' partial loss of intramolecular energy and stabilize less-stable conformations.‡ This observation has cast some doubt on the transferability of structural information determined by diffraction methods from the solid state to other phases for use in the interpretation of chemical and physical properties.

One way to evaluate the role of the crystalline field in the molecular structure of flexible molecules is to compare the conformation of molecules in different polymorphic modifications. The basic assumption underlying this approach is that the effect of crystal forces will show up more clearly where the molecule is more flexible, *i.e.* where a deformation from the 'optimum' molecular structure (that of the isolated molecule) will be energetically least expensive. For instance, since relatively large energies are required to bring about significant changes in bond distances and angles in organic molecules, structural differences between organic polymorphs are usually shown by molecules possessing extensive torsional degrees of freedom ('conformational polymorphism').

In this paper we discuss a rare example of crystal polymorphism for a high-nuclearity transition-metal carbidocarbonyl cluster, *viz.* $[Ru_6C(CO)_{17}]$. The structure of this prototypical octahedral cluster was first determined in 1969 by Sirigu *et al.*[5] from visual estimation of diffraction intensities obtained from Weissenberg photographic data. These authors were not only able to establish the essential structural features of the first binary carbonyl containing an encapsulated C(carbide) atom {the only previously known carbide cluster was $[Ru_6C(CO)_{14}(\eta^6\text{-}C_6H_3Me_3\text{-}1,3,5)]$[6]} but also to describe in detail the ligand distribution around the octahedral metal framework.

In the course of our studies of the factors determining and controlling the crystal packing of transition-metal carbonyl clusters and complexes[7] we have compared the crystal structure of some hexaruthenium arene clusters with that of the binary carbonyl parent.[8] Since the original coordinates of $[Ru_6C(CO)_{17}]$ are not available in either the original paper or in the Cambridge Crystallographic Data Base, we have made a fresh data collection and structural characterization.

Crystals of $[Ru_6C(CO)_{17}]$ were obtained as previously described.[9a] Alternatively red-brown crystals of $[Ru_6C(CO)_{17}]$ could be obtained[9b] by heating a cyclohexane or benzene solution of $[Ru_3(CO)_{12}]$[9c] at 150 °C under nitrogen. The two preparations afforded two different crystalline materials. The differences and similarities observed between the two molecular and crystal structures are compared in terms of conformational polymorphism.

The Molecular Structures of $[Ru_6C(CO)_{17}]$

In the following discussion the crystal corresponding to the 'new' structural determination will be designated form **I**, while

† *Supplementary data available:* see Instructions for Authors, *J. Chem. Soc., Dalton Trans.*, 1992, Issue 1, pp. xx–xxv.

‡ A classic example where higher-energy conformations are observed in the solid state is that of biphenyl: the angle between the two rings is 42° in the gas phase, while the 'average' molecule is planar in the solid state at room temperature and twisted 10° at 22 K; see ref. 4.

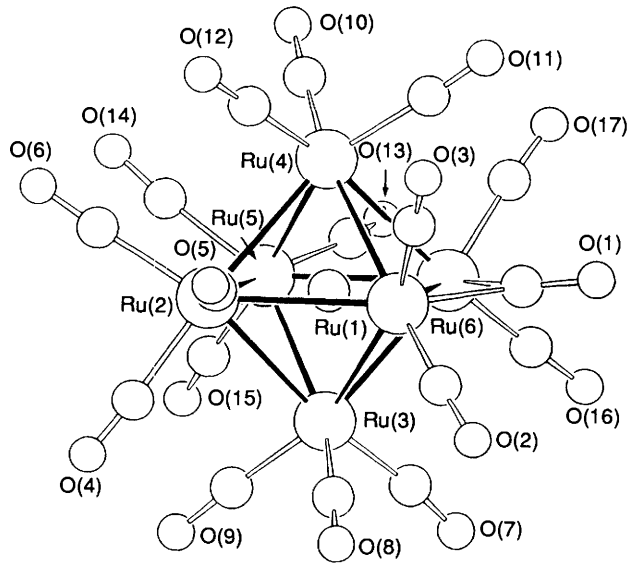

Fig. 1 View of $[Ru_6C(CO)_{17}]$ in its molecular structure **I** showing the labelling scheme. The C atoms of the CO groups bear the same numbering as the corresponding O atoms

the 'old' one will be designated form **II**. Since **II** contains 'one and a half' independent molecules in the asymmetric unit (see Experimental section), while **I** contains one single molecular unit, there are (at least in principle) three different molecular structures of $[Ru_6C(CO)_{17}]$. We will refer to these as **IIA**, **IIB** and **I**. The structure of $[Ru_6C(CO)_{17}]$ in its form **I** is shown in Fig. 1, together with the atomic labelling scheme. The three molecules are compared in Fig. 2, and the relevant structural parameters listed in Table 1.

At the *molecular level* the most relevant differences between **I**, **IIA** and **IIB** arise essentially from the rotameric conformation of the tricarbonyl units above and below the equatorial plane containing the bridging ligands, and from the pattern of terminal, bridging, and semibridging CO groups around the molecular equator. Before discussing these two aspects in detail, however, the following general considerations can be made with respect to the data in Table 1.

(*i*) The Ru–Ru bond lengths in forms **I**, **IIA** and **IIB** differ in range [**I**, 2.835(3)–2.967(3); **IIA**, 2.826(1)–2.998(1); **IIB**, 2.803(1)–2.977(1) Å] and in their average values [2.898(3), 2.893(1) and 2.885(1) Å]. The differences between corresponding bonds over the three molecular units are about ten times larger than the estimated standard deviations on the individual parameters, and, therefore, are significant and reflect physically meaningful structural differences.

(*ii*) The Ru–C(carbide) distances appear to be less variable, being, in spite of the deformations of the metal core, identical in their mean values in the three molecules (2.05 Å).

(*iii*) There is no correspondence between the Ru–Ru bond lengths and the presence of bridging ligands; the symmetrically bridged bond is much shorter in **I** [2.835(3) Å] than in **IIA** and **IIB** [2.868(1) and 2.867(1) Å]. This is actually the shortest bond in **I**, while the shortest bond in **IIB** is that opposite the bridged edge [Ru(2A)–Ru(2A′) 2.803(1) Å] and in **IIA** is located between an equatorial atom and an apex [Ru(1)–Ru(4) 2.826(1) Å].

(*iv*) The longest Ru–Ru bond is the same in all three structures and corresponds to the equatorial edge spanned by the least bent semibridging ligand [C(5)O(5) along the Ru(1)–Ru(2) edge].

Therefore, the metal–metal bonds show a great structural variation not only on passing from one crystal lattice to the other but also between the two independent molecular units in the same lattice. This overall picture is in agreement with previous observations that the metal atom frameworks in transition-metal clusters are 'soft' and adaptable to the steric and electronic demands of the ligands packed around the core and of the surrounding molecules in the lattice.[10] The tricarbonyl units do also possess some degree of structural flexibility as demonstrated by the OC–Ru–CO angles within the $(CO)_3$ cones which range from 90(1) to 93(1) in **I** and from 90.8(2) to 94.0(2)° in **II** with no easily recognizable pattern.

The differences in the distribution of the bridging ligands around the molecular equators and in the conformation of the tricarbonyl units above and below can easily be recognized from the comparative views of **I**, **IIA** and **IIB** shown in Fig. 2. The two tricarbonyl units are almost exactly staggered in **I**, while they tend towards an eclipsed conformation in **IIA** and **IIB**. Taking the equatorial bridging CO [C(1)–O(1) in Fig. 2] as reference, the limiting rotameric conformations of the two tricarbonyl units can be designated as in Scheme 1.

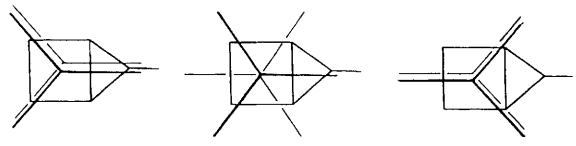

cis-cis *cis-trans* *trans-trans*

Scheme 1

Both *cis-cis* and *trans-trans* conformations have approximate *mm* symmetry, while the *cis-trans* conformation possesses *m* symmetry only. The *trans-trans* conformation is not observed. Fig. 2 clearly shows that the conformation in **I** is very close to *cis-trans*, deviating (on the average) only 7° from exact staggering of the apical CO groups, while in **IIA** and **IIB** the conformation of the $(CO)_3$ units is approximately *cis-cis*. In these latter molecules, however, the two sets of $(CO)_3$ units are tilted differently with respect to the equatorial bridging CO (see Table 1 for relevant torsion angles).

The presence of three different rotameric conformations can be taken as evidence that the tricarbonyl units lie in a rather flat potential-energy surface without well defined conformational minima. This conclusion is substantiated by the observation of a similar conformational *non-preference* in the mono- and bis-arene derivatives of $[Ru_6C(CO)_{17}]$ characterized to date. Although $[Ru_6C(CO)_{14}(\eta^6\text{-}C_6H_5Me]$,[11] $[Ru_6C(CO)_{14}(\eta^6\text{-}C_6H_3Me_3\text{-}1,3,5)]$[6,8] and $[Ru_6C(CO)_{11}(\eta^6\text{-}C_6H_3Me_3\text{-}1,3,5)_2]$[12] retain the overall CO-ligand distribution of the binary carbonyl compound (including the presence of one bridging and two semibridging CO groups), the relative conformation of the arene and of the tricarbonyl unit is staggered (*cis-trans*) in $[Ru_6C(CO)_{14}(\eta^6\text{-}C_6H_5Me)]$[11] and eclipsed (*cis-cis*) in $[Ru_6C(CO)_{14}(\eta^6\text{-}C_6H_3Me_3\text{-}1,3,5)]$.[6,8] Similarly, in the bis(arene) species $[Ru_6C(CO)_{11}(\eta^6\text{-}C_6H_3Me_3\text{-}1,3,5)_2]$ the two mesitylene ligands adopt a *cis-cis* conformation with respect to the bridging CO ligand.[12]

This may be taken as indicative that *intramolecular* electronic and/or steric effects contribute very little to the conformational choice of the ligand(s) co-ordinated to the apical ruthenium atoms. This choice is then controlled primarily at the *intermolecular level*. Along this line of thinking it is clear that the different bridging patterns around the molecular equators in **I**, **IIA** and **IIB** are also dictated by packing interactions. For instance, while the bridging ligand in **I** and **IIB** is symmetric, that in **IIA** is slightly asymmetric [2.048(4) *versus* 2.142(4) Å]. Analogously, the two equatorial semibridging ligands [C(5)–O(5) and C(13)–O(13) in **I** and **IIA**, C(5A)–O(5A) and C(5A′)–O(5A′) in **IIB**] show different degrees of asymmetry in the three molecules, with 'long' Ru···C interactions varying from 2.523(6) Å in **IIA** to 2.96(3) Å in **I**. Interestingly, while in **IIB** equivalence of the two semibridging ligands [C(5A)–O(5A), C(5A′)–O(5A′)] on the opposite edges of the Ru_4 equator is imposed by crystallographic symmetry, in **IIA**, that is in general

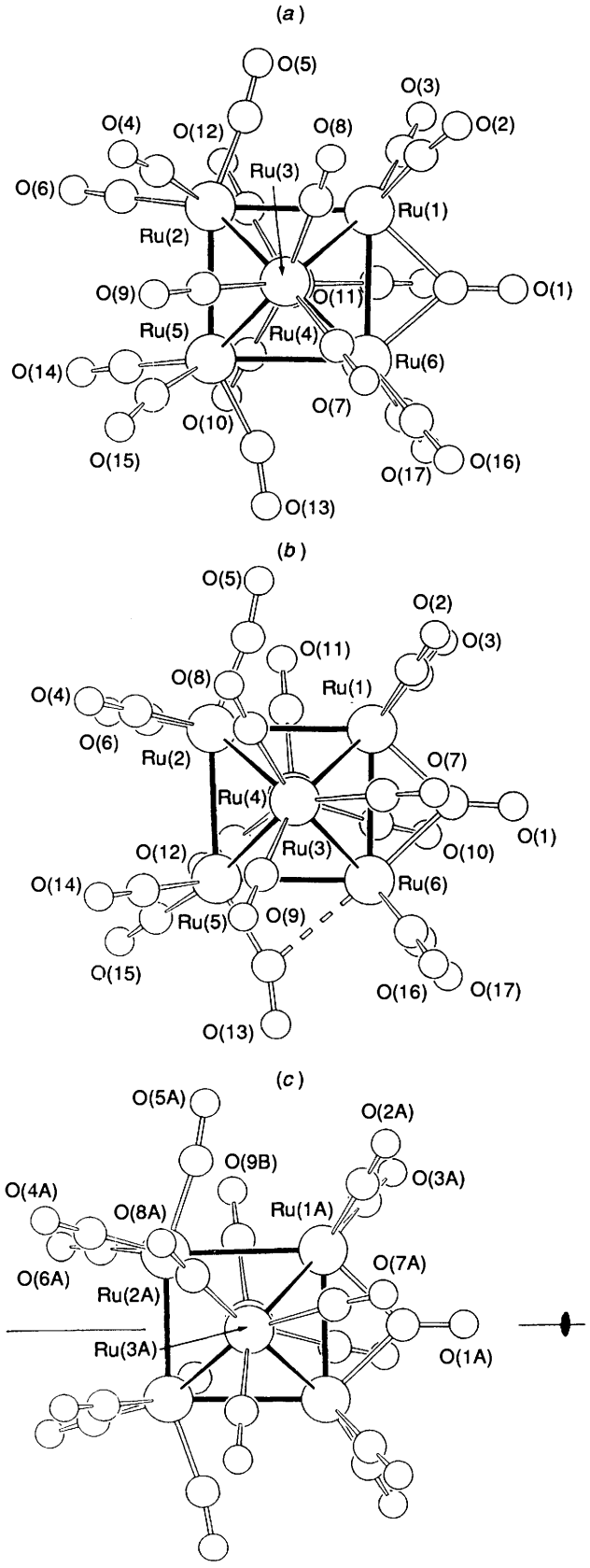

Fig. 2 Projection of structures **I** (*a*), **IIA** (*b*) and **IIB** (*c*) perpendicular to the CO-bridged equatorial plane showing the different rotameric conformations of the tricarbonyl units above and below the plane. The rotameric conformation is of the type *cis-trans* in **I**, and *cis-cis* in **IIA** and **IIB**. The different patterns of bridging, semibridging, and bent-terminal CO groups around the equatorial plane of the three molecules can also be appreciated. The C atoms of the CO groups bear the same numbering as the corresponding O atoms

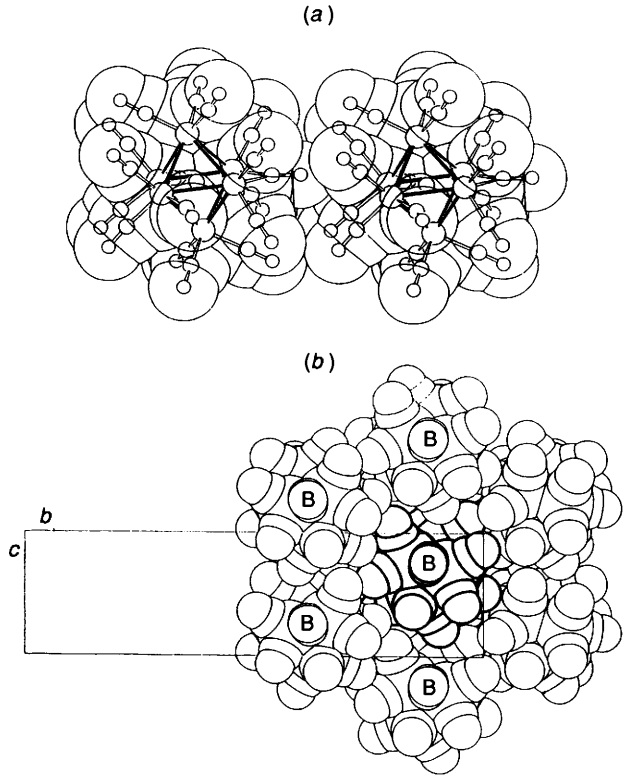

Fig. 3 (*a*) The 'head-to-tail' linkage of two consecutive molecules in the lattice of form **I**. The intermolecular interlocking is based on the insertion of the bridging ligand [C(1)–O(1) in Fig. 1] in the middle of the tetragonal cavity generated by the four terminal CO groups (4, 6, 14 and 15 in Fig. 1) of the next neighbouring molecule. (*b*) Space-filling projection of the packing distribution in the *bc* plane of form **I**; the letter B marks the bridging CO ligands and shows the 'direction' of the molecular rows parallel to the *a* axis

position, the two ligands show rather different degrees of bending [Ru–C–O angles 169.4(5) *versus* 156.8(5)°, 'long' Ru · · · C interactions 2.916(5) *versus* 2.523(6) Å, for C(5)–O(5) and C(13)–O(13), respectively].

The Crystal Structures of $[Ru_6C(CO)_{17}]$

In order to investigate the relationship between molecular organization in the lattice and molecular structure in forms **I** and **II** we need to decode the two packing patterns. This can easily be done by empirical packing potential-energy (PPE) calculations as briefly described in the Methodology section. We focus attention on the intermolecular interactions between one molecule chosen as reference (RM) and those forming the immediate surroundings and enclosing the reference one (the first neighbouring molecules, FNM, see below). While this procedure is straightforward in the case of form **I**, it is complicated by the presence of 'one and a half' independent molecules in the asymmetric unit of **II**. In the latter case the analysis of two independent molecular surroundings is required.

The fundamental packing motif in form **I** [see Fig. 3(*a*)] is constituted by trains of molecules linked 'head-to-tail' *via* insertion of the bridging ligand [C(1)–O(1) in Figs. 1 and 2(*a*)] in the middle of the cavity generated by the four terminal CO groups linked to the opposite Ru–Ru edge [carbonyls 4, 6, 14 and 15 in Figs. 1 and 2(*a*)]. These molecular trains extend along the *a* axis; each molecular row is surrounded by four rows pointing in the same direction, and by two rows pointing in the opposite direction [the 'direction' of the row is indicated by the bridging CO groups, see Fig. 3(*b*)].

Although, as mentioned above, the packing distribution in form **II** is complicated by the presence of one and half

Table 1 Comparison of some relevant structural parameters (bond lengths in Å, angles in °) of $[Ru_6C(CO)_{17}]$ in forms **I** ($P2_1/n$) and **II** ($P2/a$)

	I	IIA	IIB	
Ru(1)–Ru(2)	2.967(3)	2.998(1)	Ru(1A)–(2A)	2.977(1)
Ru(1)–Ru(3)	2.923(3)	2.855(1)	Ru(1A)–(3A)	2.896(1)
Ru(1)–Ru(4)	2.880(3)	2.826(1)	Ru(1A)–(3A′)	2.838(1)
Ru(1)–Ru(6)	2.835(3)	2.868(1)	Ru(1A)–(1A′)	2.867(1)
Ru(2)–Ru(3)	2.861(3)	2.899(1)	Ru(2A)–(3A)	2.932(1)
Ru(2)–Ru(4)	2.880(3)	2.868(1)	Ru(2A)–(3A′)	2.886(1)
Ru(2)–Ru(5)	2.901(3)	2.860(1)	Ru(2A)–(2A′)	2.803(1)
Ru(3)–Ru(5)	2.883(3)	2.925(1)		—
Ru(3)–Ru(6)	2.967(3)	2.867(1)		—
Ru(4)–Ru(5)	2.892(2)	2.946(1)		—
Ru(4)–Ru(6)	2.882(3)	2.944(1)		—
Ru(5)–Ru(6)	2.907(3)	2.858(1)		—
Ru(1)–C(99)	2.02(3)	2.026(4)		2.049(3)
Ru(2)–C(99)	2.05(2)	2.060(3)		2.062(3)
Ru(3)–C(99)	2.05(2)	2.034(3)		2.029(3)
Ru(4)–C(99)	2.04(2)	2.046(3)		—
Ru(5)–C(99)	2.09(3)	2.062(4)		—
Ru(6)–C(99)	2.07(2)	2.045(3)		—
Ru(1)–C(1)	2.10(3)	2.048(4)	Ru(1A)–C(1A)	2.070(4)
Ru(6)–C(1)	2.10(3)	2.142(4)		—
C(1)–O(1)	1.16(3)	1.154(5)	C(1A)–O(1A)	1.158(6)
Ru(2)–C(5)	1.89(3)	1.917(6)	Ru(2A)–C(5A)	1.907(5)
Ru(1) · · · C(5)	2.96(3)	2.916(5)	Ru(1A) · · · C(5A)	2.950
C(5)–O(5)	1.09(3)	1.111(8)	C(5A)–O(5A)	1.132(6)
Ru(5)–C(13)	1.90(3)	1.946(5)		—
Ru(6) · · · C(13)	2.65(3)	2.523(6)		—
C(13)–O(13)	1.17(3)	1.146(7)		—
Ru(1)–C(1)–O(1)	137(2)	139.9(4)	Ru(1A)–C(1A)–O(1A)	136.2(1)
Ru(6)–C(1)–O(1)	138(2)	133.7(4)		—
Ru(2)–C(5)–O(5)	173(2)	169.4(5)	Ru(2A)–C(5A)–O(5A)	170.4(4)
Ru(5)–C(13)–O(13)	160(2)	156.8(5)		—
Ru(6)–C(13)–O(13)	121(2)	124.9(4)		—

Dihedral angles (°)

	I	IIA
C(7)–Ru(3) · · · Ru(4)–C(10)	68.2	23.1
C(8)–Ru(3) · · · Ru(4)–C(11)	67.6	26.3
C(9)–Ru(3) · · · Ru(4)–C(12)	66.4	25.9

Dihedral angles for **IIB**

C(7A)–Ru(3A) · · · Ru(3A′)–C(7A′)	33.1
C(8A)–Ru(3A) · · · Ru(3A′)–C(9A′)	38.2

independent molecules in the asymmetric unit, it is remarkable that the 'head-to-tail' interaction, constituting the backbone of form **I**, is maintained in **II** [see Fig. 4(*a*)]. The molecules around the crystallographic two-fold axes in form **II** are linked 'head-to-tail' as those in **I**. The molecular rows in the two crystalline forms differ, however, not only in the orientation of the tricarbonyl units above and below the bridged equatorial plane, but also in a small tilting of the molecules in form **I** with respect to **II** [compare Figs. 3(*a*) and 4(*a*)]. The tilting appears to allow a more efficient molecular interpenetration along the rows in the former crystal as reflected by the shorter intermolecular separation with respect to the latter [9.19(1), and 9.335(1) Å in **I** and **II**, respectively]. In form **II** two molecular rows pointing in opposite directions are placed side by side in the unit-cell *ac* plane [see Fig. 4(*b*)].

The molecules in general position (**IIa**) do not establish 'head-to-tail' interactions, rather these molecules point their bridging CO groups towards the neighbouring rows formed by molecules of the **IIb** type, as shown in Fig. 4(*b*). In a sense the lattice of form **II** can be seen as constituted of layers of 'head-to-tail' bound molecular rows (similar to those found in form **I**) *intercalated* every two layers of molecules in different orientation.

Conclusion

We have demonstrated that $[Ru_6C(CO)_{17}]$ shows ligand isomerism in the solid state. This is not very common in the structural chemistry of transition-metal carbonyl clusters in spite of the enormous number of species characterized to date. We would argue, however, that ligand isomerism in the solid state and crystal polymorphism might be much more common for organometallic molecules possessing extensive structural non-rigidity. Other examples are those afforded by the isomeric pairs $[Ir_6(CO)_{16}]$[13] and $[Ru_6H(B)(CO)_{17}]$.[14] The former is known in two crystalline forms: one with four face-capping ligands ('red isomer') and the other with four edge-bridging ligands ('black isomer'). Both isomers have crystallographic C_2 symmetry in their crystals. It has been shown that the face-capped isomer, despite a smaller molecular volume and a less-distorted metal atom polyhedron, is less efficiently packed than the edge-bridged isomer.[7a] The case of the hydridic boride $[Ru_6H(B)(CO)_{17}]$ is also very interesting.[14] It has been recently shown [14a] that the two isomers differ essentially in the rotameric conformation of the tricarbonyl units above and below the plane containing a bridging CO (as observed in **I** and **II**) and in the location of the H(hydride) ligand.[14] It seems possible

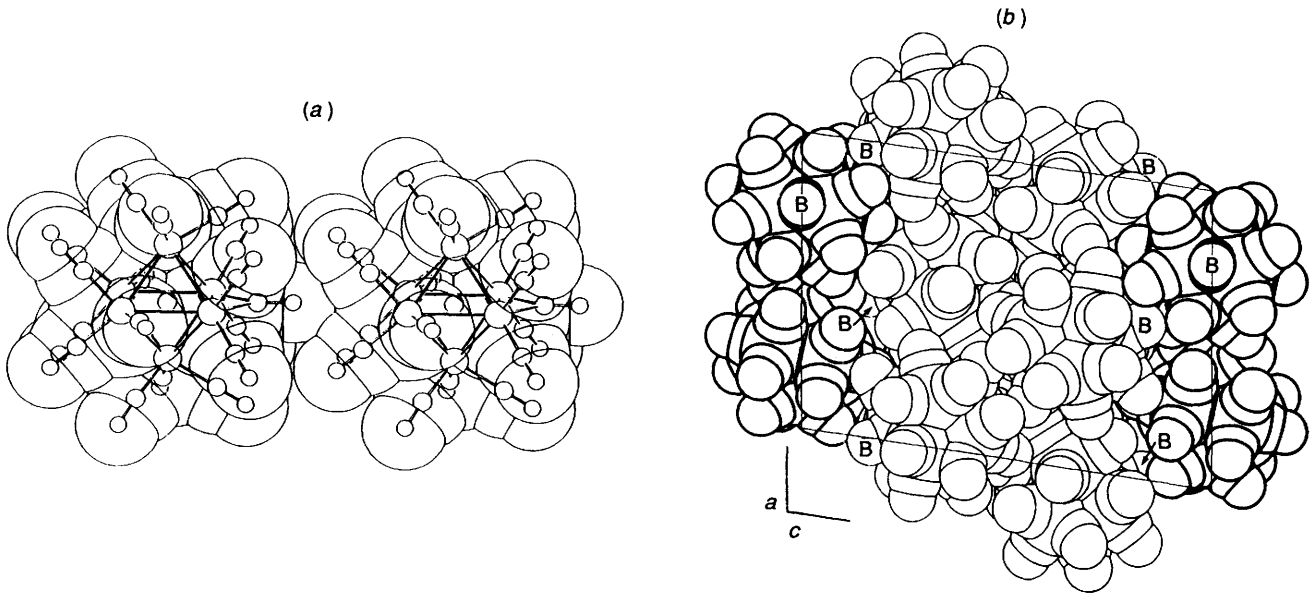

Fig. 4 (*a*) The 'head-to-tail' linkage of two consecutive molecules in the lattice of form **II** based on the insertion of the bridging ligand in the middle of the tetragonal cavity generated by four terminal CO groups [compare with the similar packing motif observed in form **I** shown in Fig. 3(*a*)]. (*b*) Space-filling projection of the packing distribution in the *ac* plane of form **II**; the letter B marks the bridging CO ligands. The rows of 'head-to-tail' molecules extend along the *b* axis, forming layers which 'sandwich' two other layers of differently oriented molecules

Table 2 Crystal data and details of measurements for forms **I** and **II** *

	I	**II**
Crystal size (mm)	0.1 × 0.16 × 0.1	0.12 × 0.12 × 0.15
Space group	$P2_1/n$	$P2/a$
a/Å	9.19(1)	17.668(2)
b/Å	32.043(9)	9.335(1)
c/Å	9.598(4)	24.057(7)
β/°	111.93(3)	97.96(2)
U/Å^3	2622	3929
Z	4	6
F(000)	2032	3048
D_c/g cm^{-3}	2.77	2.78
μ(Mo-Kα)/cm^{-1}	31.35	31.39
2θ range/°	5–50	5–56
ω-Scan width/°	1.5	0.7
Requested counting $\sigma(I)/I$	0.01	0.02
Prescan rate/° min^{-1}	5	8
Maximum scan time/s	90	100
Measured reflections	4755	10 288
Unique observed reflections [$I > 2\sigma(I)$] (n)	2764	7656
No. of parameters (m)	370	557
Absorption correction range	0.49–1.0	0.86–1.00
R, R'	0.076, 0.079	0.023, 0.028
S	2.79	1.20
K, g	3.0, 0.0012	1.0, 0.001

* Details in common: $C_{18}O_{17}Ru_6$, M_r 1094.6; crystal system, monoclinic; prescan acceptance, $\sigma(I)/I = 0.5$; $R' = \Sigma[(F_o - F_c)w^{\frac{1}{2}}]/\Sigma F_o w^{\frac{1}{2}}$, where $w = K/[\sigma(F) + |g|F^2]$; $S = \Sigma[(F_o - F_c)/\sigma]^2/(n - m)$.

to conclude that, in all these cases, the different molecular structures represent, very likely, the result of *different* compromises between crystal energy and conformational energy.[7a,10c]

We have also shown that structural parameters concerning the metal core, though known with much greater accuracy than those involving the light atoms, are affected enormously by packing forces. The differences between chemically equivalent sets of bond distances, for instance, are one order of magnitude larger than the estimated standard deviations on each individual value. This should warn against a too confident use of small differences in bond lengths and angles to derive information on chemical behaviour, or to associate directly bond length to bond strength. Crystal-packing analysis, on the other hand, further demonstrates the effect of the molecular organization in the lattice on the 'average' geometry of the molecules. It seems possible to conclude that different molecular structures are observed because the energy difference between the various ligand distributions is comparable to the energy difference between the crystalline forms. On these premises it can be predicted that *structurally non-rigid* transition-metal cluster molecules, such as those showing extensive ligand fluxionality in solution, will be optimum candidates for studies of organometallic polymorphism.

Table 3 Fractional atomic coordinates for form I

Atom	x	y	z	Atom	x	y	z
Ru(1)	−0.2539(2)	−0.1646(1)	−0.2054(2)	C(8)	0.0269(34)	−0.1465(9)	0.1076(28)
Ru(2)	0.0455(2)	−0.1712(1)	−0.2544(2)	O(8)	0.0432(26)	−0.1654(6)	0.2021(23)
Ru(3)	0.0112(2)	−0.1093(1)	−0.0541(2)	C(9)	0.2278(29)	−0.0983(7)	0.0344(27)
Ru(4)	−0.2367(2)	−0.1425(1)	−0.4896(2)	O(9)	0.3607(25)	−0.0903(8)	0.0930(29)
Ru(5)	0.0131(2)	−0.0840(1)	−0.3416(2)	C(10)	−0.2425(28)	−0.1118(9)	−0.6625(33)
Ru(6)	−0.2810(2)	−0.0797(1)	−0.2942(2)	O(10)	−0.2497(28)	−0.0945(9)	−0.7680(25)
C(99)	−0.1179(26)	−0.1262(7)	−0.2710(26)	C(11)	−0.4632(27)	−0.1492(9)	−0.5733(27)
C(1)	−0.4306(30)	−0.1199(8)	−0.2379(31)	O(11)	−0.5888(21)	−0.1527(6)	−0.6250(24)
O(1)	−0.5547(22)	−0.1186(6)	−0.2330(27)	C(12)	−0.2014(22)	−0.1945(8)	−0.5655(25)
C(2)	−0.2750(32)	−0.1856(8)	−0.0371(26)	O(12)	−0.1812(22)	−0.2266(6)	−0.6100(24)
O(2)	−0.2913(25)	−0.1958(9)	−0.0742(26)	C(13)	−0.1154(29)	−0.0365(8)	−0.4188(29)
C(3)	−0.3843(28)	−0.2095(10)	−0.3043(29)	O(13)	−0.1549(22)	−0.0032(6)	−0.4692(31)
O(3)	−0.4614(23)	−0.2362(6)	−0.3667(27)	C(14)	0.1039(29)	−0.0911(8)	−0.4927(30)
C(4)	0.2429(27)	−0.1801(10)	−0.0852(42)	O(14)	0.1459(23)	−0.0951(8)	−0.5859(26)
O(4)	0.3595(22)	−0.1838(8)	0.0041(25)	C(15)	0.1954(33)	−0.0535(8)	−0.2352(32)
C(5)	−0.0211(27)	−0.2254(8)	−0.2279(30)	O(15)	0.2939(21)	−0.0301(8)	−0.1821(22)
O(5)	−0.0457(22)	−0.2580(6)	−0.2136(26)	C(16)	−0.3209(30)	−0.0345(10)	−0.1912(31)
C(6)	0.1523(32)	−0.1879(9)	−0.3889(35)	O(16)	−0.3495(28)	−0.0060(8)	−0.1294(30)
O(6)	0.2067(25)	−0.1983(9)	−0.4682(26)	C(17)	−0.4442(27)	−0.0598(10)	−0.4676(29)
C(7)	−0.0344(28)	−0.0618(8)	0.0451(29)	O(17)	−0.5444(21)	−0.0469(6)	−0.5671(22)
O(7)	−0.0487(28)	−0.0350(7)	0.1143(23)				

Table 4 Fractional atomic coordinates for form II

Atom	x	y	z	Atom	x	y	z
Ru(1)	0.596 04(2)	0.170 22(3)	0.257 57(1)	O(13)	0.419 0(2)	0.528 2(5)	0.398 8(2)
Ru(2)	0.662 08(2)	0.124 39(3)	0.377 88(1)	C(14)	0.533 9(3)	0.237 4(5)	0.471 5(2)
Ru(3)	0.500 04(2)	0.094 32(3)	0.339 16(1)	O(14)	0.519 2(2)	0.177 5(5)	0.509 2(1)
Ru(4)	0.661 37(2)	0.399 23(3)	0.324 55(1)	C(15)	0.608 4(4)	0.476 0(6)	0.458 8(2)
Ru(5)	0.559 26(2)	0.337 64(3)	0.408 54(1)	O(15)	0.636 4(4)	0.557 0(6)	0.489 3(2)
Ru(6)	0.494 49(2)	0.379 00(3)	0.294 10(1)	C(16)	0.387 7(2)	0.356 3(4)	0.279 7(2)
C(99)	0.579 1(2)	0.249 9(3)	0.333 2(1)	O(16)	0.323 9(2)	0.344 9(4)	0.273 1(2)
C(1)	0.513 1(2)	0.296 0(4)	0.214 1(2)	C(17)	0.479 8(2)	0.571 4(4)	0.266 1(2)
O(1)	0.485 4(2)	0.317 8(5)	0.168 6(1)	O(17)	0.469 1(2)	0.680 1(4)	0.250 4(2)
C(2)	0.569 0(3)	−0.005 0(5)	0.218 6(2)	Ru(1A)	0.244 37(2)	0.392 14(3)	0.058 88(1)
O(2)	0.554 0(2)	−0.108 5(4)	0.195 4(2)	Ru(2A)	0.244 89(2)	0.073 24(3)	0.057 61(1)
C(3)	0.666 3(3)	0.205 9(5)	0.206 7(2)	Ru(3A)	0.365 82(2)	0.238 70(3)	0.015 14(1)
O(3)	0.709 0(3)	0.224 3(5)	0.176 0(2)	C(99A)	0.25	0.235 2(4)	0.0
C(4)	0.659 8(3)	−0.013 0(6)	0.435 9(2)	C(1A)	0.25	0.552 2(5)	0.0
O(4)	0.659 6(3)	−0.091 8(5)	0.471 5(2)	O(1A)	0.25	0.676 2(4)	0.0
C(5)	0.709 8(3)	0.001 9(6)	0.329 0(2)	C(2A)	0.307 7(2)	0.476 5(4)	0.121 0(2)
O(5)	0.743 8(3)	−0.076 2(6)	0.307 9(2)	O(2A)	0.343 0(2)	0.525 9(4)	0.159 1(1)
C(6)	0.750 6(3)	0.202 4(6)	0.419 1(2)	C(3A)	0.160 7(2)	0.480 3(5)	0.085 2(2)
O(6)	0.804 5(3)	0.244 7(6)	0.444 5(2)	O(3A)	0.111 7(2)	0.538 0(5)	0.100 6(2)
C(7)	0.430 9(3)	0.037 1(5)	0.275 3(2)	C(4A)	0.311 5(2)	−0.079 9(5)	0.084 5(2)
O(7)	0.388 1(2)	0.002 5(4)	0.237 9(2)	O(4A)	0.350 5(2)	−0.171 0(4)	0.101 0(2)
C(8)	0.528 5(3)	−0.097 2(5)	0.359 5(2)	C(5A)	0.235 1(3)	0.139 5(5)	0.131 2(2)
O(8)	0.541 4(3)	−0.214 6(4)	0.367 9(2)	O(5A)	0.227 9(2)	0.159 2(4)	0.176 6(1)
C(9)	0.420 5(3)	0.100 7(6)	0.385 3(2)	C(6A)	0.163 0(2)	−0.059 0(5)	0.049 9(2)
O(9)	0.371 7(2)	0.101 5(7)	0.411 3(2)	O(6A)	0.115 2(2)	−0.139 9(4)	0.044 6(2)
C(10)	0.646 0(2)	0.531 5(7)	0.264 7(2)	C(7A)	0.415 1(2)	0.412 3(4)	0.041 6(2)
O(10)	0.641 3(2)	0.607 5(5)	0.227 3(2)	O(7A)	0.446 4(2)	0.513 2(4)	0.053 9(2)
C(11)	0.758 5(3)	0.343 8(6)	0.306 8(2)	C(8A)	0.429 8(3)	0.127 2(4)	0.067 9(2)
O(11)	0.816 0(2)	0.311 0(5)	0.296 1(2)	O(8A)	0.471 1(2)	0.065 5(4)	0.099 6(2)
C(12)	0.705 8(3)	0.545 3(6)	0.374 2(2)	C(9A)	0.432 1(2)	0.220 6(5)	−0.041 4(2)
O(12)	0.734 3(3)	0.635 5(5)	0.400 9(2)	O(9A)	0.469 5(2)	0.211 3(5)	−0.075 1(2)
C(13)	0.468 9(3)	0.456 9(6)	0.390 2(2)				

Experimental

Crystals of form **II** were obtained as previously reported.[9a] The complex $[Ru_3(CO)_{12}]$ was placed in a Burghoff autoclave (250 cm^3) with heptane (150 cm^3). The autoclave was flushed with N_2, then pressurized to 30 atm (*ca.* 3.04 × 10^6 Pa) ethylene. The vessel was heated at 150 °C for 4 h. After cooling for 24 h, crystals of $[Ru_6C(CO)_{17}]$ (0.38 g) were obtained. These were recrystallized from dichloromethane–hexane.

Red-brown crystals of form **I** were prepared by thermolysis at 150 °C of $[Ru_3(CO)_{12}]$ in benzene or cyclohexane under a nitrogen atmosphere. The $[Ru_3(CO)_{12}]$ was synthesised according to Braca *et al.*[9c] In a typical experiment, $[Ru_3(CO)_{12}]$ (0.1 g) and benzene (10 cm^3) were introduced in a glass vial and placed in a rocking autoclave containing benzene and heated at 150 °C for 12 h. The autoclave was slowly cooled, the vial recovered and the crystals (0.07 g, yield 81.8%) separated from the solution were filtered off, washed with pentane, dried under vacuum and characterized (Found: C, 20.10; Ru, 55.20. Calc. for $C_{18}O_{17}Ru_6$: C, 19.75; Ru, 55.40%). IR (C_6H_{12}): 2066vs, 2047vs, 2002vw and 1844vw cm^{-1}, in agreement with the bands reported by Piacenti *et al.*;[9b] (KBr pellet) 2080 (sh), 2039vs, 2028s, 1990s, 1979s, 1856w and 1822m cm^{-1}.

The IR spectra were recorded using a Perkin-Elmer model 1760 FTIR spectrophotometer. Elemental analyses were performed using a Perkin-Elmer model 245 elemental analyser. The ruthenium content was determined by weighing after thermal decomposition of the crystals under a reducing atmosphere.

Crystal Structure Determination.—All measurements were made on an Enraf-Nonius CAD-4 diffractometer equipped with a graphite monochromator (Mo-Kα radiation, λ = 0.710 69 Å). The intensities were collected in ω–2θ scan mode at room temperature. Crystal data and details of measurements are summarized in Table 2. The structures were solved by using direct methods followed by Fourier difference syntheses and least-squares refinements. Scattering factors for neutral atoms were taken from ref. 15*a*. For all calculations the SHELX 76 program was used.[15b] An absorption correction was applied by the Walker and Stuart method[15c] once complete structural models were available and all atoms refined isotropically. All atoms were treated anisotropically. Fractional atomic coordinates for forms **I** and **II** are reported in Tables 3 and 4, respectively.

Additional material available from the Cambridge Crystallographic Data Centre comprises H-atom coordinates, thermal parameters and remaining bond distances and angles.

Crystal-packing Investigation: Methodology.—Our approach to crystal-packing problems has its roots in the pairwise atom–atom potential-energy method of Kitaigorodsky.[16a,b] The application of the method to transition-metal complexes and clusters has been discussed previously and needs only a brief summary in the context of this study. For more details the reader is addressed to refs. 3 and 7. Use is made of the expression packing potential energy[16a] $= \Sigma_i\Sigma_j[A \exp(-Br_{ij}) - Cr_{ij}^{-6}]$, where r_{ij} represent the non-bonded atom–atom intermolecular distances. Index i in the summation runs over all atoms of one molecule (chosen as reference molecule) and j over the atoms of the surrounding molecules distributed according to crystal symmetry. A cut-off of 15 Å was adopted in our calculations. The values of the coefficients A–C used were taken from the literature[16b] and discussed in previous papers.[3] The results of packing potential energy calculations are used to select the first-neighbouring molecules (FNM) among the molecules surrounding the one chosen as reference (RM) on the basis of its contribution to the packing potential energy. It should be stressed that this procedure is used only as a convenient means of investigating the molecular environment within the crystalline lattice without any pretentions of obtaining 'true' (or even approximate) crystal potential-energy values. All calculations were carried out with the aid of the computer program OPEC;[17] SCHAKAL 88[18] was used for the graphical representation of the results.

Acknowledgements

Financial support by Ministero della Università e della Ricerca Scientifica e Tecnologica is acknowledged; D. B., F. G. and B. F. G. J. also wish to acknowledge NATO for a travel grant. The SERC and British Petroleum are acknowledged by P. J. D.

References

1 J. Bernstein, *Organic Solid State Chemistry*, ed. G. R. Desiraju, Elsevier, Amsterdam, 1987, p. 471; J. Bernstein and A. T. Hagler, *J. Am. Chem. Soc.*, 1978, **100**, 673.
2 W. C. McCrone, *Physics and Chemistry of the Organic Solid State*, eds. D. Fox, M. M. Labes and A. Weissberger, Interscience, New York, 1963, vol. 1, p. 725.
3 D. Braga and F. Grepioni, *Organometallics*, 1991, **10**, 1254; D. Braga, F. Grepioni, B. F. G. Johnson, J. Lewis, C. E. Housecroft and M. Martinelli, *Organometallics*, 1991, **10**, 1260; D. Braga and F. Grepioni, *Organometallics*, 1992, **11**, 1256.
4 W. R. Busing, *Acta Crystallogr., Sect. A*, 1983, **39**, 340.
5 A. Sirigu, M. Bianchi and E. Benedetti, *Chem. Commun.*, 1969, 596.
6 R. Mason and W. R. Robinson, *Chem. Commun.*, 1968, 468; see also ref. 8.
7 (*a*) D. Braga and F. Grepioni, *Acta Crystallogr., Sect. B*, 1989, **45**, 378; (*b*) D. Braga, F. Grepioni and P. Sabatino, *J. Chem. Soc., Dalton Trans.*, 1990, 3137; (*c*) D. Braga, F. Grepioni, P. Sabatino and A. Gavezzotti, *J. Chem. Soc., Dalton Trans.*, 1992, 1185; (*d*) D. Braga and F. Grepioni, *Organometallics*, 1991, **10**, 2563; (*e*) D. Braga and F. Grepioni, *Organometallics*, 1992, **11**, 711.
8 D. Braga, F. Grepioni, B. F. G. Johnson, C. Hong and J. Lewis, *J. Chem. Soc., Dalton Trans.*, 1991, 2559.
9 (*a*) B. F. G. Johnson, J. Lewis, S. W. Sankey and K. Wong, *J. Organomet. Chem.*, 1980, **191**, C3; (*b*) F. Piacenti, M. Bianchi and E. Benedetti, *Chem. Commun.*, 1967, 775; (*c*) G. Braca, G. Sbrana and P. Pino, *Chim. Ind. (Milan)*, 1968, **50**, 121.
10 (*a*) V. G. Albano, D. Braga and F. Grepioni, *Acta Crystallogr., Sect. B*, 1989, **45**, 60; (*b*) D. Braga and F. Grepioni, *J. Organomet. Chem.*, 1987, **336**, C9; (*c*) V. G. Albano and D. Braga, *Accurate Molecular Structures*, eds. A. Domenicano and I. Harghittay, Oxford University Press, 1991 and refs. therein.
11 L. J. Farrugia, *Acta Crystallogr., Sect. C*, 1988, **44**, 997.
12 D. Braga, F. Grepioni, S. Righi, P. J. Dyson, B. F. G. Johnson, P. J. Bailey and J. Lewis, *J. Chem. Soc., Dalton Trans.*, 1992, 2121.
13 L. Garlaschelli, S. Martinengo, P. L. Bellon, F. Demartin, M. Manassero, M. Y. Chiang, C. Y. Wei and R. Bau, *J. Am. Chem. Soc.*, 1984, **106**, 6664.
14 (*a*) S. M. Draper, C. E. Housecroft, A. K. Keep, D. M. Matthews, X. Song and A. L. Rheingold, *J. Organomet. Chem.*, 1992, **423**, 241; (*b*) F. Hong, T. J. Coffy, D. A. McCarthy and S. G. Shore, *Inorg. Chem.*, 1989, **28**, 3284.
15 (*a*) *International Tables for X-Ray Crystallography*, Kynoch Press, Birmingham, 1975, vol. 4, pp. 99–149; (*b*) G. M. Sheldrick, SHELX 76, Program for Crystal Structure Determination, University of Cambridge, 1976; (*c*) N. Walker and D. Stuart, *Acta Crystallogr., Sect. B*, 1983, **39**, 158.
16 (*a*) A. I. Kitaigorodsky, *Molecular Crystal and Molecules*, Academic Press, New York, 1973; (*b*) A. J. Pertsin and A. I. Kitaigorodsky, *The Atom–Atom Potential Method*, Springer, Berlin, 1987; (*c*) A. Gavezzotti and M. Simonetta, *Chem. Rev.*, 1981, **82**, 1; (*d*) K. Mirsky, *Proceedings of the International Summer School on Crystallographic Computing*, Delft University Press, Twente, 1978, p. 169.
17 A. Gavezzotti, OPEC, Organic Packing Potential Energy Calculations, University of Milano, 1983; see also *J. Am. Chem. Soc.*, 1983, **195**, 5220.
18 E. Keller, SCHAKAL 88, Graphical Representation of Molecular Models, University of Freiburg, 1988.

Received 14*th February* 1992; *Paper* 2/00786J